J Mater Sci (2006) 41:7894–7901
DOI 10.1007/s10853-006-0871-4

Tensile properties of iron-based P/M steels with ferrite + martensite microstructure

A. Güral · S. Tekeli · T. Ando

Received: 13 August 2005 / Accepted: 22 November 2005 / Published online: 20 September 2006

Abstract The effect of intercritical heat treatments on the tensile properties of iron-based P/M steels was investigated. For this purpose, atomized iron powder (Ancorsteel 1000) was admixed with 0.3 wt.% graphite powder. Tensile test specimens were cold pressed at 700 MPa and sintered at 1120 °C for 30 min under pure argon gas atmosphere. After sintering, ~20% pearlite volume fraction in a ferrite matrix was obtained. To produce coarse ferrite + martensite microstructures, the sintered specimens were intercritically annealed at 724 and 760 °C and quenched in water. To obtain fine ferrite + martensite microstructures, the sintered specimens were first austenitized at 890 °C and water-quenched to produce a fully martensitic structure. These specimens were then intercritically annealed at 724 and 760 °C and re-quenched. After the intercritical annealing at 724 and 760 °C and quenching, martensite volume fractions were ~ 18% and 43%, respectively, in both the coarse- and fine-grained specimens. Although the intercritically annealed specimens exhibited higher yield and tensile strength than the as-sintered specimens, their elongation values were lower. Specimens with a fine ferrite + martensite microstructure showed high yield and tensile strength and ductility in comparison to specimens with a coarse ferrite + martensite microstructure. The strength values of specimens increased with increasing martensite volume fraction.

A. Güral · S. Tekeli (✉)
Materials Division, Technical Education Faculty,
Gazi University, 06500 Besevler-Ankara, Turkey
e-mail: stekeli@gazi.edu.tr

T. Ando
Department of Mechanical, Industrial and Manufacturing Engineering, Northeastern University,
334 Snell Engineering Centre, Boston 02115, USA

Introduction

Powder metallurgically (P/M) processed steel components have attracted much attention as candidates for replacing wrought steels in many applications due to their low cost, high performance and ability to be processed to near-net shape [1]. However, the most important problems encountered in P/M steels are porosity and heterogeneous microstructures produced during sintering which directly affect the mechanical properties of P/M steels. Porosities impair the static and dynamic mechanical properties of P/M steels as they reduce the effective load bearing section and give rise to a notch effect [2, 3]. Generally, the properties of P/M steels can be improved either by admixing alloying elements at high concentrations or by applying heat treatments. To produce a martensite structure in P/M steels after quenching, an adequate level of alloying element, especially carbon, must be maintained. However, pre-alloying the powder with carbon reduces the pressing capability of powders. For this reason, carbon should be admixed as an alloying element. Graphite is used in P/M steels as the carbon source.

While hard phases or structures generally increase the yield and tensile strength of P/M steels, softer phases or structures tend to improve impact toughness and ductility. In this study, it was aimed to produce martensite as the hard phase and ferrite as the soft phase in the microstructures. To produce these phases

in P/M steels, the sintered steels were subjected to intercritical heat treatments as applied frequently to low alloy ingot steels [4–6].

Intercritical annealing between the Ac_1 and Ac_3 temperatures produces a mixture of ferrite and austenite in a low-alloy hypoeutectoid steel. The austenite, upon quenching, transforms to islands of martensite, producing a ferrite + martensite dual-phase structure in the steel. An increase in intercritical annealing temperature results in an increase in austenite (martensite) volume fraction but also in a decrease in martensite carbon content. The yield and tensile strengths increase with increasing martensite volume fraction, but at the expense of ductility. Also, for a fixed constant carbon content, the hardness of martensite increases as the martensite volume fraction decreases [7]. While the intercritical annealing temperatures determine the martensite (austenite) volume fraction and carbon content, the microstructure before intercritical annealing determines the final martensite morphology [8, 9]. Thus, by controlling the shape, size, amount and distribution of the martensite in the dual-phase microstructure, the desired combination of strength and ductility is obtained.

When dual phase steels were first invented, studies were focused more on their formability properties. Today, however, it is clear that other mechanical properties such as impact toughness, fatigue, tensile and torsion properties can be improved through optimizing the shape, size, amount and chemical composition of the martensite in ferrite matrix [8, 10–14]. The aim of the present study was to produce ferrite + martensite microstructures having different martensite volume fractions and morphologies in low carbon P/M steels through intercritical heat treatments and to investigate the effects of these microstructures on tensile properties.

Experimental procedures

In this study, atomized iron (Ancorsteel 1000, Hoeganaes, USA) and natural graphite (Alfa Aesar, Germany) powders were used. The properties of Ancorsteel 1000 iron powder are given in Table 1. Specimens were prepared by directly mixing 0.3 wt.% graphite with iron powder. To this iron and graphite powder mixture 0.5 wt.% Zn stearate was added as a lubricant.

Dog bone shaped tensile specimens were cold pressed at 700 MPa as suggested in ASTM E 8M standards. To increase the pressing capability of powders, 10 wt.% Zn stearate dissolved in ethanol was applied onto the die walls. Specimens were sintered at 1120 °C for 30 min under pure Argon gas (99.999%) atmosphere. The rate of heating to and cooling from the sintering temperature was both kept at 4 °C min^{-1}. A schematic illustration of the heat treatments applied to the sintered tensile test specimens is shown in Fig. 1. Heat treatments were carried out in a vertical furnace which enabled rapid quenching of the test specimens. In order to produce coarse ferrite + martensite microstructures after sintering, the specimens were directly annealed at intercritical annealing temperatures of 724 and 760 °C for 16 min and quenched in water. Specimens with this heat treatment were coded as CM. To produce fine ferrite + martensite microstructures, other sintered specimens were first austenitized at 890 °C for 12 min and water-quenched to produce a fully martensitic structure. These fully martensitic specimens were then intercritically annealed at 724 and 760 °C and re-quenched in water. Specimens with these heat treatments were coded as FM.

Macrohardness values of each specimen were measured with an Instron Wolpert Vickers tester using a 5 kg load. Microhardness values of the phases in the microstructures were determined with a Shimadzu HMV-2 Vickers tester using a 50 g load. All hardness measurements were carried out at least at 15 different areas of each specimen and average values were taken.

Tensile tests were conducted using a universal tensile testing machine (Instron 5500) at an initial strain rate of 1.3×10^{-3} s^{-1}. Results of the tensile test were determined as true stress and true strain.

For microstructural investigation, specimens were ground and polished by using usual metallographic procedures. To reveal the microstructures 3% nital was used. Different etching times ranging from 5 to 15 s

Table 1 Properties of Ancorsteel 1000 iron powder

Composition (wt.%) (w/o)									
C	O	N	S	P	Si	Mn	Cr	Cu	Ni
< 0.01	0.14	0.002	0.018	0.009	< 0.01	0.20	0.07	0.10	0.08
Sieve distribution (w/o)									
Micrometers	+250	–250/+150	–150/+45	–45					
U.S. standard mesh	(+60)	(–60/+100)	(–100/+325)	(–325)					
	Trace	10	68	22					

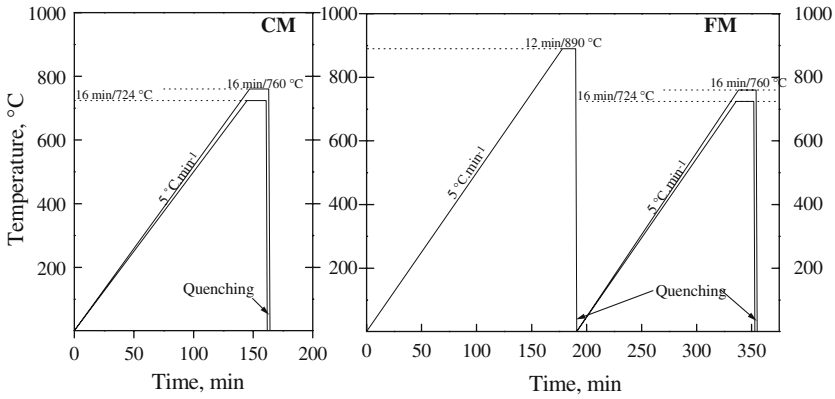

Fig. 1 Schematic illustration of heat treatments applied to P/M specimens

were chosen for specimens having different graphite contents and at the end of these periods, the specimens were washed with running water and rinsed with methyl alcohol to remove the etchant from the surfaces. The mean linear intercept method was used to determine the amount and size of phases. Measurements were carried out at least at 10 different areas in each specimen and average values were obtained. The area used for each measurement for the calculation of martensite volume fraction was $450 \times 600\ \mu m^2$. A scanning electron microscope (SEM JSM 6360) was used to characterize the microstructure and fracture surface of the specimens.

Results and discussion

Microstructure and hardness

The microstructure of the as-sintered specimen before the intercritical annealing is shown in Fig. 2. In this specimen, pearlite colonies with typical lamellar morphology nucleated and grew from the prior austenite boundaries. The 4 °C min^{-1} cooling rate from the sintering temperature provided enough time for the formation of pearlitic structures. The pearlite volume fraction of the as-sintered microstructure is about 20%.

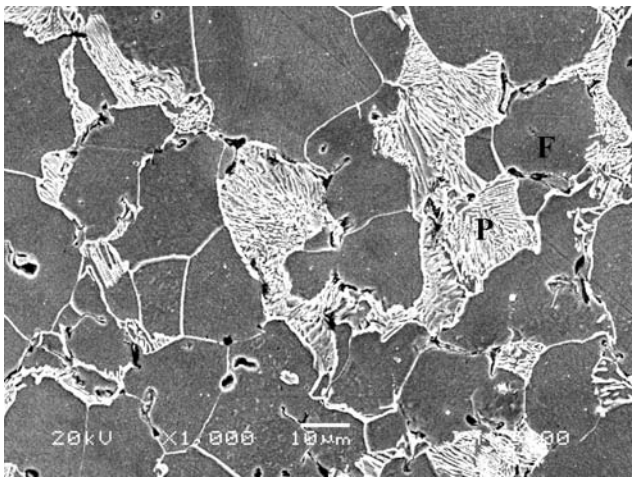

Fig. 2 Microstructure of as-sintered specimen before intercritical heat treatment (F: ferrite; P: pearlite)

The microstructures after the intercritical heat treatments are shown in Fig. 3. In the CM specimens, coarse martensite islands were formed (Fig. 3a, b). During intercritical annealing, austenite nucleates primarily at the Fe_3C/ferrite interface and forms by taking the place of the pearlite colonies. Subsequently, depending on the annealing time, it grows into the ferrite grains [15, 16]. In the FM specimens martensite islands are dispersed more uniformly in the microstructure (Fig. 3c, d). Also, both the ferrite grains and martensite islands are finer in these specimens than in the CM specimens. However, in this study martensite morphology was not needle-like as seen in dual phase ingot steel structures [17]. When a specimen with an initially martensite microstructure is intercritically annealed, austenite nucleates and grows at martensite lath boundaries [8]. The areas left by austenite remain as ferrite. Subsequent quenching transforms the austenite into martensite with fine and needle-like morphology [8, 12]. In this study, the initial microstructure of the FM specimens before intercritical annealing was also martensite. However, the martensite structure was over tempered before reaching the intercritical annealing temperatures due to the slow heating rate (4 °C min^{-1}) (martensite decomposes to ferrite and cementite as temperature increases. This cementite would further spheroidize and coarsen under the slow heating conditions). Thus, martensites after intercritical heat treatment had fine equiaxed morphology instead of needle-like shape. The martensite volume fractions after quenching from 724 and 760 °C were ~18% and 43%, respectively, in both the CM and FM specimens.

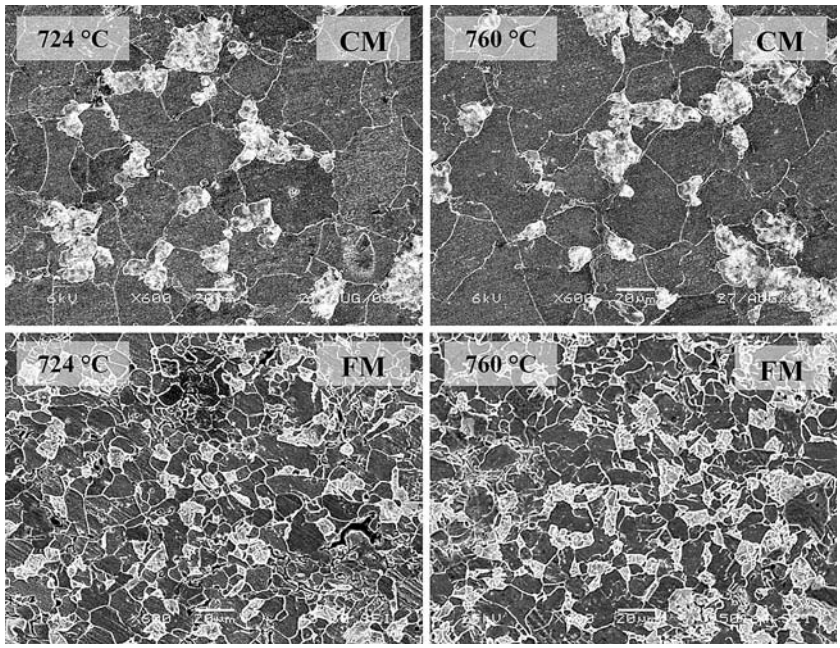

Fig. 3 Martensite morphology in CM and FM specimens (white area is martensite; dark gray area is ferrite)

The hardness values of the specimens are given in Table 2. The macrohardness values of the as-sintered specimens were lower than those of the CM and FM specimens. In the CM and FM specimens, the increase in intercritical annealing temperature increased the martensite volume fraction and thus there was a slight increase in their macrohardness values. As known an increase in intercritical annealing temperature, results in a decrease in carbon content of austenite (martensite after quenching). Thus the microhardness values of martensite are lower for the specimens that were intercritically annealed at 760 °C. The microhardness of the ferrite around martensite increased slightly with increasing martensite volume fraction (Table 2). It is believed that this increase in ferrite hardness is due to formation of mobile dislocations in the ferrite adjacent to the martensite [18].

Tensile properties

The stress–strain curves of the sintered and intercritically annealed specimens (CM, FM) are shown in Fig. 4. Although, the yield and tensile strengths of the as-sintered specimen were very low, its ductility values were higher than those of the intercritically annealed specimens. Furthermore, the as-sintered specimens showed a clear yield point. The volume fraction, dispersion and morphology of the martensite also affected the tensile behavior of the specimens. With the increase in martensite volume fraction, yield and tensile strength increased while ductility decreased. Similar relations were also observed by the present authors in the intercritically annealed and conventionally heat treated (quenched + tempered) low carbon P/M steels [19].

Previous studies have also shown that [8, 9] a small mean distance between fine martensite islands gives rise to decreased dislocation mobility in the ferrite, thereby increasing the yield strength. The yield/tensile strength and ductility values of the FM specimens were higher than those of the CM specimens. However, the ductility values in those specimens were not as high as those of dual phase ingot steels [5, 8, 12]. Specimens fractured just after the maximum tensile strength was reached. Thus, the uniform elongation and total elon-

Table 2 Properties of sintered and heat treated specimens

Samples	Intercritical annealing temperature (°C)	Martensite volume fraction (%)	True yield stress (MPa)	True tensile stress (MPa)	Fracture elongation (%)	Hardness (HV5)	Microhardness (HV0.05)	
							Martensite	Ferrite
Sintered	–	–	112 ± 11	239 ± 13	10.8 ± 1,79	97 ± 3	–	–
CM	724	18	261 ± 18	427 ± 15	5.1 ± 0,47	206 ± 5	838 ± 43	142 ± 6
	760	43	319 ± 19	496 ± 16	4.7 ± 0,35	215 ± 7	496 ± 6	162 ± 7
FM	724	18	325 ± 16	443 ± 22	7.5 ± 0,56	212 ± 10	747 ± 33	154 ± 16
	760	43	334 ± 21	538 ± 19	6.9 ± 1,71	219 ± 8	434 ± 18	166 ± 11

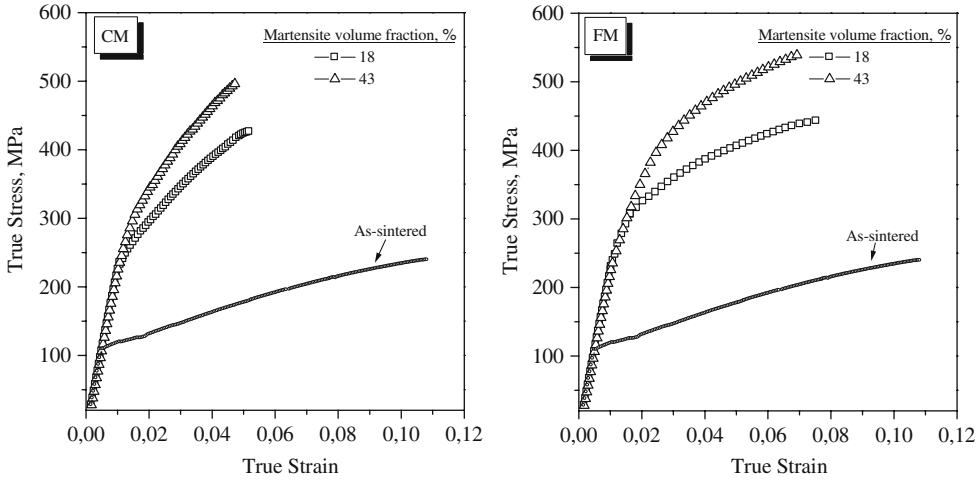

Fig. 4 Effect of martensite volume fraction on true stress–strain curves of CM and FM specimens

gation values were nearly the same. Moreover, no clear necking was observed in the fracture region of the specimens. The absence of necking was caused by the pores in the sintered material. The loads applied to P/M specimens in a tensile test are carried by the bonds occurring between sintered powder particles [20]. As a consequence, in the FM and CM specimens, micro-necking was observed between powder particles (Fig. 5).

In P/M materials the strength and ductility are controlled by the amount of effective load-bearing section. The ductility of P/M materials with porosity is low since plastic deformation occurs mostly at necks between particles [1]. The martensite islands formed in the intercritically annealed specimens increased strain hardening and decreased ductility. The highest strain-hardening rate was observed in the FM specimens with a fine ferrite + martensite microstructure.

In this study, all the specimens with ferrite + martensite microstructures exhibited a continuous yielding behavior, which is characteristic of dual phase steels. This continuous yielding was caused by the mobile dislocations formed in the ferrite as the austenite islands transform to martensite during quenching after the intercritical annealing [21]. For a fixed martensite volume fraction the fine-grained dual phase FM specimens showed higher tensile and yield strength than the coarse-grained CM specimens. This can be explained by the fine martensite and ferrite grain size and the short mean distance between martensite islands [22].

The stress–strain curves obtained in this study are similar to those that were found in previous P/M steel studies in the literature [23]. As known it is very difficult to get full densities in P/M steels through single act pressing and sintering. In general, the mechanical properties of P/M steels that cannot be fully densified are affected by the properties, amount and morphology of the second phase (bainite, martensite, etc.) in the structure. The present study has also shown that the amount, morphology and the hardness of the martensite in the ferrite matrix affected the tensile properties.

As in dual phase ingot steels, ferrite volume fraction and martensite size also determined the ductility in this study. Ferrite volume fraction decreased while the martensite volume fraction increased, which resulted in a decrease in ductility. The ductility values of the fine-grained FM specimens were higher than those of the coarse-grained CM specimens. This can be attributed

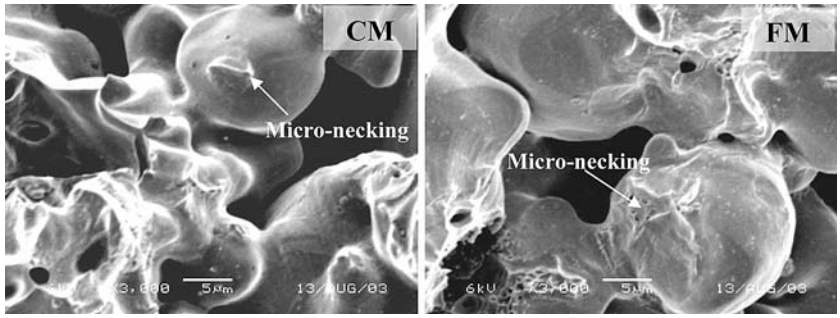

Fig. 5 Micronecking formation between powder particles in CM and FM specimens

to the formation of microvoids during tensile test [24, 25]. In specimens with coarse martensite islands, the amount of interconnected martensites are more, which causes microvoid enlargement due to easy fracture of martensite even at low strains and thus low ductility values (Fig. 6).

An increase in strength with an increase in martensite volume fraction is one of the general properties of dual phase steels [22]. The tensile properties are also affected by the chemical composition of the martensite (for example carbon content) [26, 27]. Davies [28] stated that martensite volume fraction has greater effects on the tensile properties of dual phase steels than the chemical composition of the martensite. During the tensile test, microplastic regions can be seen at the inter-particle necks near the pores even at low stresses. This causes early fracture [29] of specimens. These plastic regions spread into the matrix and may induce a pore volume growth with a corresponding decrease in the effective load-bearing section [29, 30]. In addition, depending on the pore irregularity and matrix deformability, microcracks may also occur at pore edges and spread more readily during tensile test [29, 31–33]. In this study, the matrix phase was ferrite. The inter-particle neck regions may be ductile or brittle depending on the phase that exists there. If a ductile ferrite grain exists at a pore edge, microcracks may be arrested by the ferrite grains. However, if there is martensite at a pore edge, pores can create a notch effect on martensite promoting fracture. This causes ductility to decrease as happened in the CM specimens.

Hard regions like martensite islands in the microstructure of P/M steels increase strain-hardening rate and decrease ductility [34]. Also, ductility may be decreased by bainite formation in the microstructure [35]. Coarse and adjacent martensite islands cause the formation of inhomogeneous deformation. Similarly if martensite islands are adjacent to each other as they were in the CM specimen (Fig. 3a, b), microvoid enlargement that causes fracture occurs even at lower plastic strains [36]. It was stated that formation and enlargement of microvoid occur with either fracture of martensite islands or de-cohesion of martensite/ferrite interface [37].

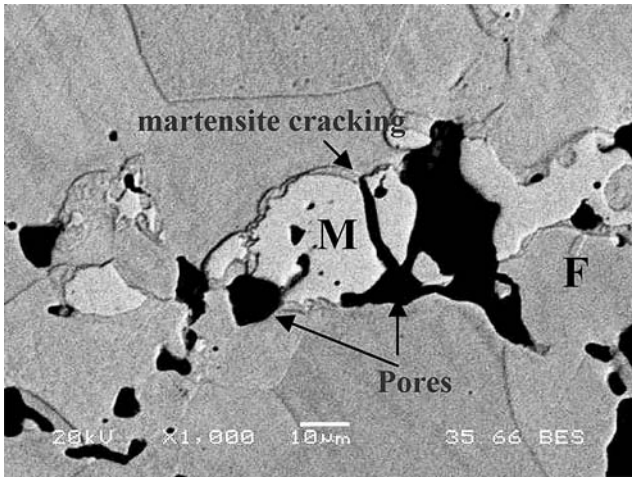

Fig. 6 Microvoid formation due to the martensite cracking in CM specimen (F: ferrite; M: martensite)

In the CM specimens, martensite islands are considered to have formed generally between sintered powder particles. This may be supported by the observation that microcrack formation in the early stage of deformation took place at the coarse martensite adjacent to the pores in the microstructure. Consequently, the ductility values of these specimens were lower than those of the fine-grained FM specimens. However, in the FM specimens, because of the homogenous dispersion of fine martensite islands within the microstructure, martensite islands were less likely to be adjacent to the pores (Fig. 3c–d). Also, in these specimens, microcracking might be delayed because microvoids at the ferrite–martensite interface are less likely to be adjacent to the pores. Thus, relatively high ductility values may be obtained even at a higher deformation rate. A number of researchers [8, 12] have shown that fine-grained dual-phase microstructure produced from a fully martensitic initial microstructure leads to better tensile properties than coarse-grained dual-phase microstructures produced from a coarse ferrite + pearlite microstructure when compared at the same martensite volume fraction. In the FM specimens, microcrack propagation might have been prevented by the interaction of micro voids with each other. Microvoids that occur due to deformation can combine with pre-existing pores in the structure of P/M steels. This accelerates microcrack formation at pores. In P/M steels, heterogeneously dispersed microstructures decrease ductility, yield strength and strain-hardening rate. However, while hard regions (such as martensite) in the microstructure increase yield strength and strain-hardening rate, ductility decreases [23].

Figures 7 and 8 present the SEM images of fracture surfaces after tensile tests. In the as-sintered specimen, fracture surface showed microdimples occurring locally at sinter necking (Fig. 7). The fracture surfaces of coarse-grained CM specimens were cleavage and predominantly dimple type (Fig. 8a, b). In the literature, it is stated that in dual phase steels, coarse-grained martensite islands crack more easily than fine-grained martensite islands [27]. In this study, cleavage areas

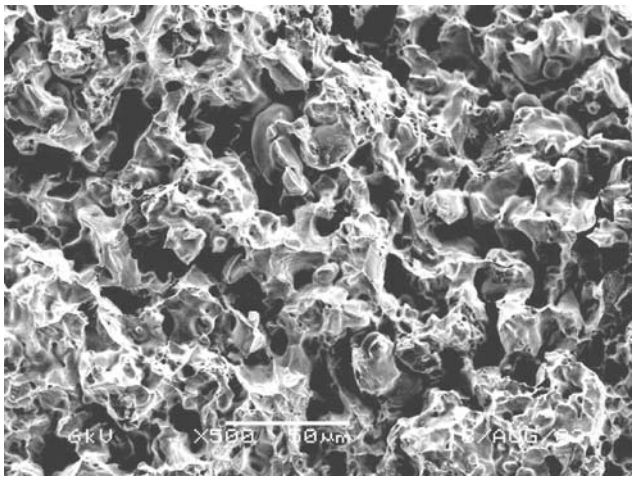

Fig. 7 Fracture surface of as-sintered specimen

after tensile test were clearly seen in the coarse-grained CM specimens. Coarse and contiguous martensites cracked at the early stage of deformation. Thus it is considered that microcracks in the martensite and ferrite caused cleavage fracture. With an increase of intercritical annealing temperature, martensite volume fraction increases while the carbon content of martensite decreases, causing the hardness of martensite islands to decrease. However, despite this hardness decrease, the coarse-grained CM specimens annealed at 760 °C still showed cleavage fracture areas. This can be attributed to increased contiguity of martensite islands due to the increased martensite volume fraction.

In the fine martensite dispersed FM specimens, cleavage type areas were not observed on the fracture surfaces after tensile testing (Fig. 8c, d). The fine martensite particles were well separated from each other, keeping the fracture path predominantly in the ferrite. This is reflected by the observation of dimple fracture. Also in these specimens local dimple fractures occurred between powder particles (grain boundaries).

Conclusions

The effect of intercritical heat treatment on tensile properties of 0.3 wt.% graphite added iron-based powders were investigated. The results are as follows:

1. In the as-sintered specimens, pearlite colonies with typical lamellar morphology nucleated and grew from the prior austenite boundaries. The yield and tensile strength of the as-sintered specimen was low but its ductility values were higher than those of intercritically annealed specimens. The sintered specimens showed a clear yield point.
2. After intercritical heat treatments, coarse martensite microstructures at the coarse ferrite grain boundaries were produced in the specimens with an initial microstructure of ferrite + pearlite. Homogeneously dispersed equiaxed martensite in the ferrite matrix was produced in the specimens with an initial microstructure of fully martensitic.
3. In intercritically annealed specimens, tensile properties were affected by volume fraction, dispersion and morphology of martensite. With increasing martensite volume fraction, the yield

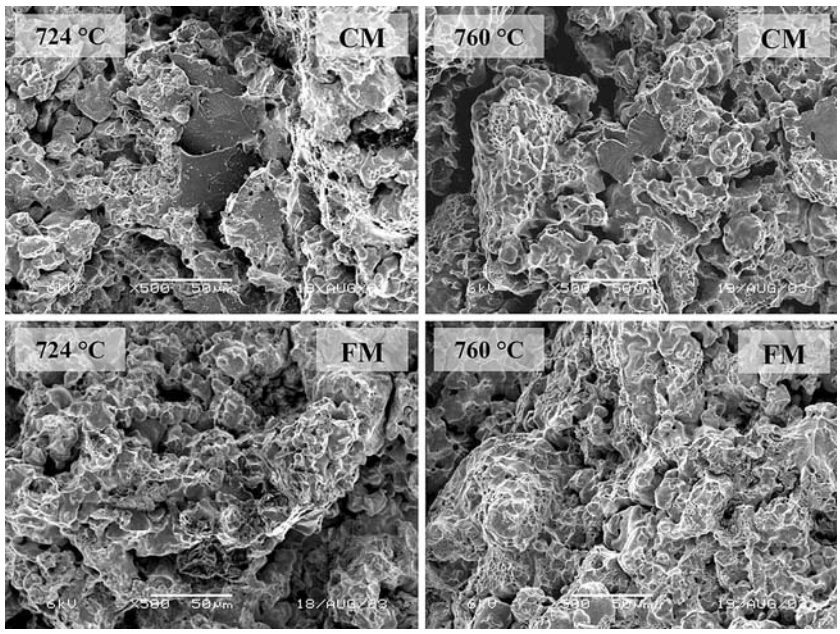

Fig. 8 Fracture surface of CM and FM specimens tensile tested after intercritical annealing heat treatment

and tensile strength increased but ductility values decreased. Higher strength and ductility values were obtained in specimens with fine ferrite + martensite microstructure.

4. The fracture surfaces of coarse-grained ferrite + martensite specimens were a mixture of cleavage and dimple type. In fine martensite dispersed specimens, cleavage type areas were not observed on the fracture surfaces after tensile testing.

Acknowledgements The authors are grateful to the DPT (the State Planning Organization of Turkey) for the financial support given under project number 2002K120250 and to Northeastern University, USA, for the use of laboratory facilities.

References

1. German RM (1998) Powder metallurgy of iron and steel. Willey, USA, pp 34
2. Danninger H, Spoljaric D, Weiss B (1997) Int J Powder Metall 33:43
3. Straffelini G, Fontanari V, Molinari A (1999) Mater Sci Eng A 260:197
4. Sun S, Pugh M (2000) Mater Sci Eng A 276:167
5. Tavares SSM, Pedroza PD, Teodósio JR, Gurova T (1999) Scr Mater 40(8):887
6. Lis J, Morgiel J, Lis A (2003) Mater Chem Phys 81:466
7. Sarwar M, Priestner R (1996) J Mater Sci 31:2091
8. Kim NJ, Nakagawa AH (1986) Mater Sci Eng 83:145
9. Cai X-L, Garratt-Reed AJ, Owen WS (1985) Metall Trans A 16:543
10. Aksoy M, Karamıs MB, Evin E (1996) Wear 19(2):428
11. Ahn YS, Kim HD, Byun TS, Oh YJ, Kim GM, Hong JH (1999) Nucl Eng Des 194(2–3):161
12. Bayram A, Uğuz A, Ula M (1999) Mater Characterization 43(4):259
13. Kim KJ, Lee CG, Lee S (1997) Scr Mater 38(1):27–32
14. Lis J, Lis AK, Kolan C (2005) J Mater Process Technol 162–163:350
15. Speich GR, Demarest VA, Miller RL (1981) Metall Trans A 12:1419
16. Garcia CI, Deardo AJ (1980) Metall Trans A 12A:521
17. Kim KJ, Lee CG, Lee S (1997) Scr Mater 38(1):27
18. El-Sesy IA, El-Baradie ZM (2003) Mater Lett 25:580
19. Tekeli S, Güral A (2005) Mater Sci Eng A 406:172
20. D'Armas H, Llanes L, Peñafiel J, Bas J, Anglada M (2000) Mater Sci Eng A 277:291
21. Mondal DK, Dey RM (1992) Metall Trans A 149A:173
22. Speich GR (1981) Physical metallurgy of dual-phase steel. Metall Soc of AIME, pp 3–45
23. Chawla N, Murphy TF, Narasimhan KS, Koopman M, Chawla KK (2001) Mater Sci Eng A 308:180
24. Jeong WC, Kim CH (1988) Metall Trans A 19(2):309
25. Ahmad E, Manzoor T, Ali KL, Akhter JI (2000) J Mater Eng Perform 9(3):306
26. Eldis GT (1979) In: Kot RA, Morris JW (eds) Structure and properties of dual phase steels. AIME, New York, pp 202–220
27. Speich RG, Miller RL (1979) In: Kot RA, Morris JW (eds) Structure and properties of dual-phase steels. AIME, New York, pp 145–182
28. Davies RG (1979) In: Davenport AT (ed) Formable HSLA and dual-phase steels. Warrendale PA, AIME, pp 25–40
29. Straffelini G, Molinari A (2002) Mater Sci Eng A 334:96
30. Spitzig WA, Smelser RE, Richmond O (1988) Acta Metall 36(5):1201
31. Exner HE, Pohl D (1978) Powder Metall Int 10(4):193
32. Dudrova E, Kabatova M (2004) Proc. Vienna PM Word Conf (EPMA) 3:193–198
33. Chawla N, Deng X (2005) Mater Sci Eng A 390:98
34. Chawla N, Polasik S, Narasimhan KS, Koopman M, Chawla KK (2001) Int J Powder Metall 37:49
35. Danninger H, Spoljaric D, Weiss B (1997) Int J Powder Metall 33:43
36. Chen HC, Cheng GH (1989) J Mater Sci 24:1991
37. Sidjanin L, Miyasato S (1989) Mater Sci Technol 5(12):1200